CONCEPTUAL MAGNET DESIGNS FOR MAX 4^{U}

H. O. C. Duarte*, K. Åhnberg, L. Roslund, MAX IV Laboratory, Lund, Sweden
A. Vorozhtsov†, European Organization for Nuclear Research, Geneva, Switzerland

Abstract

The MAX 4^{U} project aims to reduce the natural horizontal emittance of the MAX IV 3 GeV storage ring from 328 pm rad to less than 75 pm rad. A key constraint for the new lattice design is the preservation of the 7-bend achromat structure layout. Each cell is implemented as a single magnet block, which includes an integrated dipole, removable quadrupole pole tips, and stand-alone sextupoles and octupoles. This configuration imposes strict limitations on the level of intervention possible within each block. This contribution presents conceptual magnetic designs and initial crosstalk studies.

INTRODUCTION

The MAX IV 3 GeV storage ring lattice (hereafter referred to as the *standard lattice*), through the MAX 4^{U} project [1, 2], is undergoing an upgrade to reduce the natural horizontal emittance from the present 328 pm · rad to less than 75 pm · rad. The project is currently in the TDR phase [3], and the most recent lattice design (TDR_1) delivers 65 pm · rad emittance.

In order to keep the upgrade intervention cost-effective and fast, several constraints were put in place: keep the vacuum chamber profile and therefore the magnet aperture of ϕ25 mm; use magnet blocks [4], and preserve their height and layout. Each cell is realised as two halves of a magnet block. Their machining includes complete dipoles and correctors, quadrupole pole roots, and grooves for their coils. Additional grooves are milled for stand-alone sextupoles and octupoles [4]. Quadrupole pole tips, sextupole and octupoles are removable. This integrated design ensures mechanical stability and tight alignment tolerances and streamlines installation.

This paper presents conceptual magnet designs for the TDR_1 lattice with emphasis on magnetic performance, integration constraints, and cross-talk effects.

DESIGN METHODOLOGY

The magnet strengths required for the MAX 4^{U} lattice exceed the capabilities of some of the standard-lattice magnets (SLM). However, the reduced dynamic aperture of the MAX 4^{U} lattices (compared to that of the existing MAX IV 3 GeV ring) allows for a smaller good field region (GFR), whose radius was reduced from 10 mm to 7 mm. The improved field quality in this reduced GFR [5] allows to pursue narrower pole tips while still achieving about ±1 unit field quality inside the GFR.

* henrique.caiafa_duarte@maxiv.lu.se
† formerly at MAX IV Laboratory

We increase the magnet strength limits by: i) narrowing the pole tips; ii) widening of the pole roots, to the potential detriment of coil size and heat load; iii) employing Permendur as the pole tips material instead of low-carbon steel. As an example of (i) and (ii), Fig. 1 compares the 2D pole tip profiles of a quadrupole magnet. Solution (iii) has so far been kept as a last resort, and ARMCO is considered for the designs presented here. Electromagnetic (resistive) magnets are considered in this paper, while permanent-magnet-based solutions are being explored within the RF 2.0 project [6].

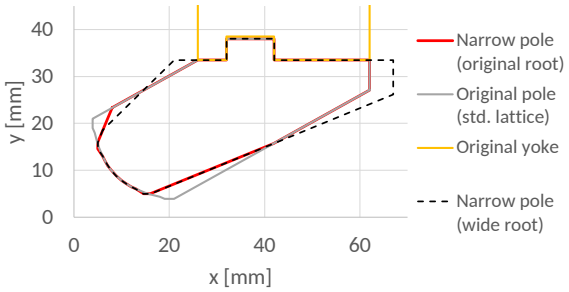

Figure 1: 2D sketch (quarter symmetry) of quadrupole pole tips: original (solid grey); narrow but keeping original root width (solid red) and widening the root (dashed black). Part of the original yoke (solid yellow) is shown as reference.

The electromagnetic designs were performed using OPERA-2D and 3D [7] and CST Studio Suite [8]. To improve mesh homogeneity, an arc or toroidal surface (for the 2D or 3D simulations) was created on the GFR boundary surrounding the ideal orbit point or path, respectively. Field maps were exported for post processing, where multipolar expansion was performed on the polar basis [5] neglecting the longitudinal fields in 3D analysis.

ELECTROMAGNETIC DESIGN

The SLM correctors and octupoles can be used for the TDR_1 lattice. 3D stand-alone EM designs have been developed for the dipoles (D2), quadrupoles (Q1 and Q2), reverse bends (R2) and sextupoles (S1, S2, S3 and S4) of the TDR_1 lattice. The most stringent families for each of these designs are shown in Table 1. No challenges are expected in designing the remaining families, D1 and R1. They are excited at a level below their SLM counterparts.

The results indicate that the required field strengths can be achieved by the proposed models, with R2 being the most constricted design. It is asymmetric, so some R2 parameters in the table refer to the halves on the inner and outer sides of the ring circumference. Not shown here, The Q1 and Q2 designs employ the narrow pole geometry (wide root), as depicted by Fig. 1.

Table 1: Magnet parameters for MAX 4^U designs, where I_c is the conductor current, L_{mag} the magnetic length, and T_{rise} the temperature rise for 2 bar nominal water pressure drop and two cooling circuits per magnet (exception is 4 for Q1). In parenthesis is the value for the corresponding SLM. The 10% safety margin is considered for the excitation level.

Parameter	**D2 (DIP)**	**Q1 (QFend)**	**R2 (QF)**	**S4 (SFo)**
Integrated Strength	0.607 (0.524) T m -10.511 (-8.537) T	13.02 (10.06) T	9.079 (6.654) T -39.46 (0) mT m	364.4 (191.53) T/m
L_{mag} [mm]	991.9 (998.1) 983.4 (987.3)	243.3 (243.3)	142.5 (143.2) 157.5 (NA)	102.1 (103.4)
I_c [A]	141.9 (121.6)	118.7 (73.9)	146.7 (74.4)	100.3 (66.1)
Bore radius [mm]	13.50 (14.00)	12.50 (12.50)	14.84 inner, 9.60 outer (12.50)	12.50 (12.50)
# of Turns/coil	54 (54)	29 (39)	43 inner, 18 outer (39)	19 (15)
Efficiency [%]	94.3 (98.0)	96.7 (89.1)	88.4 (79.6)	97.0 (96.8)
T_{rise} [°C]	8.15 (5.98)	6.39 (11.34)	14.85 (8.91)	8.96 (2.98)
Power/magnet [W]	1701.3 (1238.9)	975.1 (511.8)	1003.9 (514.6)	468.7 (168.1)

Dipoles

D2 was the least modified design compared to its SLM counterpart. Only the field clamps (simplified design) and pole profile were modified, to excite a higher gradient-to-dipole ratio. The simulation result is shown in Fig. 2. The pole-face strips [4] will be redesigned.

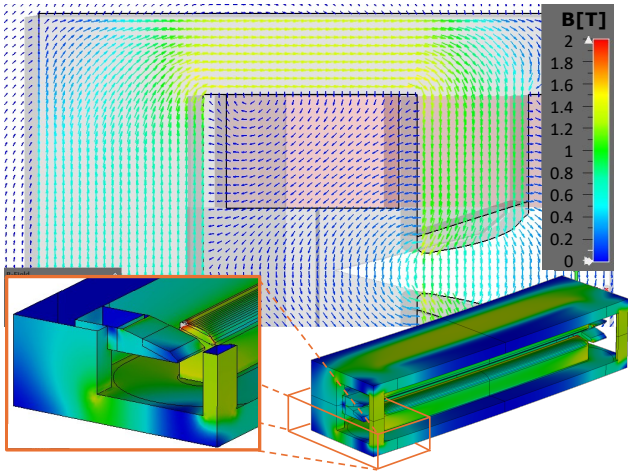

Figure 2: Collage of the stand-alone D2 simulation result at nominal excitation. B-field in vector (background) and magnitude (bottom) formats. The zoomed picture (bottom left) details the field clamp and the pole.

Reverse Bends

R2 was designed using a script that calculates the bore radii of two hyperbolae tangent to the horizontally shifted aperture circle. In this way, the air gap is minimised. The corresponding number of turns for the coil on each side was rounded from the calculated value for the resulting bore radii. Then, the radii were finely adjusted to correspond to an integer number of turns. After the 3D calculations, another iteration on the 2D design was necessary to compensate for the difference between dipole and quadrupole magnetic length. The final magnetic centre shift was of 3.86 mm. Figure 3 shows the final simulation result. for the nominal excitation level. There, the efficiency is 94.5 %, but quickly decreases to 88.4 % when it is pushed to 10 % higher excitation as in Table 1.

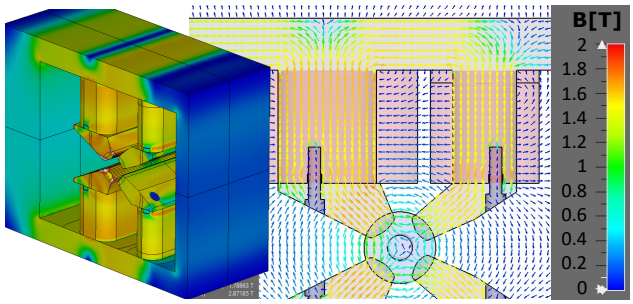

Figure 3: Stand-alone R2 model result for B-field magnitude (LHS) and vector (RHS) at nominal excitation. In the latter, as reference, are the mesh refinement region (outer) and GFR (inner) circles, concentric to the beam position.

A trim coil is also foreseen on the outer root (RHS in the figure) to allow a ±10 % dipole field variation for a fixed gradient. This range generates about ±150 Units sextupole content due to the asymmetry of the design.

Sextupoles

All sextupole families have the same design (Fig. 4). The pole tips were narrowed from 10 to 7 mm and the pole roots widened from 10 or 20 to 24 mm.

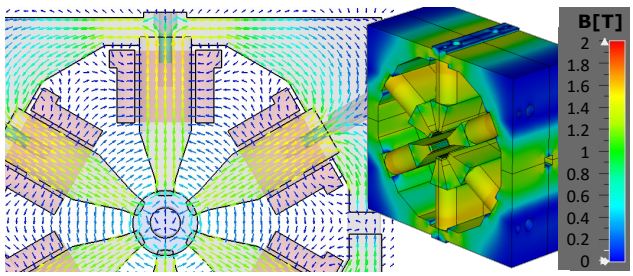

Figure 4: Stand-alone S4 model result for B-field magnitude (RHS) and vector (LHS) at nominal excitation. In the latter, as reference, are the mesh refinement region (outer) and GFR (inner) circles, concentric to the beam position.

CROSS-TALK STUDIES

Due to the proximity between magnets, magnetic cross-talk is significant and must be evaluated. The two most critical configurations have been studied: D2 between S3s and S4 between R2s. Figure 5 overlays the model for each of the two complete configurations and the magnitude of the resulting B-field in iron for the nominal excitation of the magnets.

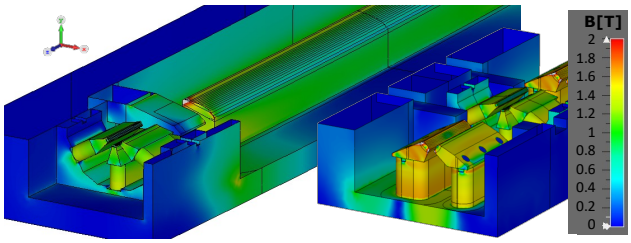

Figure 5: Collage of the two different complete crosstalk model (bottom half) results: longitudinal-half portion of D2 with field clamp and S3 on both ends (LHS model); R2s and block protrusions on both ends of S4 (RHS).

In the following studies, we split the longitudinal s-axis at the midpoint of the drift space between the magnets according to the lattice model. Then, a multipole decomposition was performed on each half to quantify cross-talk contamination in units. We compare the results of three methods: i) superposing the results of two stand-alone models; ii) using the complete model, but each magnet powered at a time with the other off, then superposing the results; iii) using the complete model with simultaneous excitation. From (i) and (ii), one can understand how much the stand-alone magnet is impacted by the insertion in the block. From (ii) and (iii), we can verify that the crosstalk is in the linear regime.

Dipole Between Sextupoles

From the results presented in Fig. 6, S3 is most affected by the return flux of D2 with an unwanted integrated dipole content of 33.74 μT · m. In addition, when S3 is inserted in that position in the block, the sextupole strength is reduced by 6.19%. This must be compensated for in the stand-alone model. The slice position requires further investigation, since a small portion of the sextupole fringe field (6.77 T/m integrated) goes to the D2 slice.

Sextupole Between Reverse Bends

Figure 7 shows that S4's slice inherits a small portion of R2's integrated dipole and gradient – 0.99% and 0.16%, respectively. Whilst the block protrusions between magnets act as shield (as seen by the blue tail on the LHS), there is not much more space available to narrow the slot and thus increase such an effect. This is due to the space required to instal a beam position monitor.

Regarding higher order multipoles, only R2 is significantly affected. The return flux of the sextupoles over the asymmetric iron path of R2 drives contents within ±4 units.

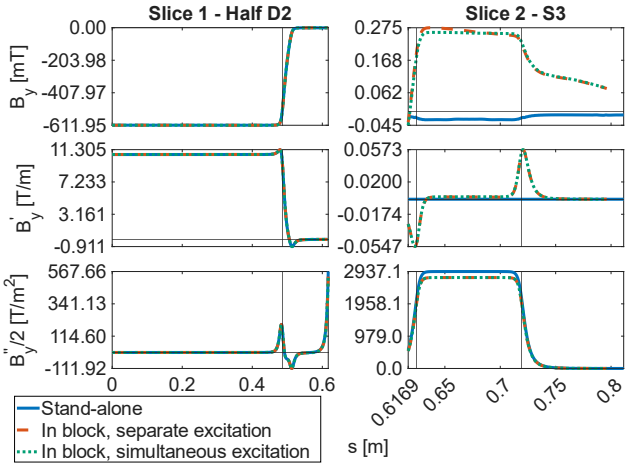

Figure 6: Dipole, quadrupole and sextupole field content (row-wise, respectively) of the cross talk between half D2 (LHS plots) and adjacent S3 (RHS plots). Are compared results for: the superposition of stand-alone models (solid blue), the superposition of the models in the block, individually excited (dashed orange) and the complete model with simultaneous excitation (dotted green). As reference, the y- axis zero-crossing line and the x-axis lines for the pole-endface locations are included.

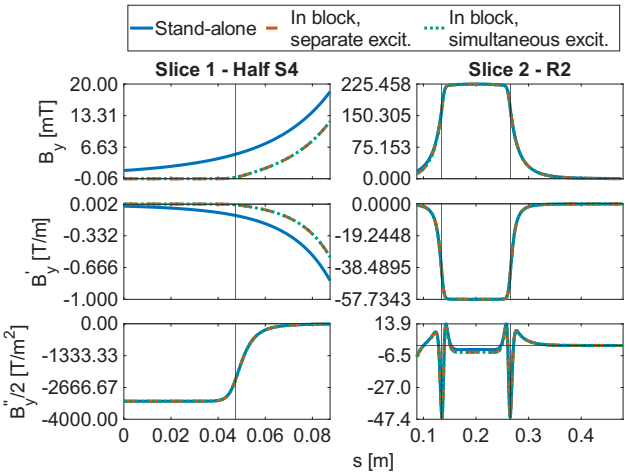

Figure 7: Cross talk between half S4 (LHS plots) and adjacent R2 (RHS plots). See Fig. 6 for the description of the curves.

CONCLUSION AND FUTURE WORK

Conceptual magnet designs for MAX 4^U have been presented that achieve the required strengths and field quality.

A prototyping programme is foreseen to validate the design, verify field quality, quantify cross-talk effects, and validate thermal and mechanical performance.

Cross-talk effects have been identified as a critical aspect of the design. The impact of the non-considered multipoles will be incorporated in the beam dynamics lattice model.

ACKNOWLEDGEMENT

We thank Lars-Johan Lindgren and Pedro F. Tavares for fruitful discussions about magnet design and methodology.

REFERENCES

[1] E. Al-Dmour *et al.*, "MAX 4^{U}: an upgrade of the MAX IV 3 GeV ring", in *Proc. IPAC'25*, Taipei, Taiwan, pp. 752–755, Nov. 2025. doi:10.18429/JACoW-IPAC2025-MOPS061

[2] "MAX 4^{U} Conceptual Design Report". https://www.maxiv.lu.se/wp-content/plugins/sharepoint-plugin/ajax/downloadFile.php?site_id=MAXIV&version_series_id=34&repository_id=0df38c7e-6f77-43c7-8ab8-bd7153273666

[3] E. Al-Dmour *et al.*, "MAX 4^{U}: an upgrade of the MAX IV 3 GeV ring", Presented at IPAC'26, Deauville, France, May 2026, paper THI2M01, this conference.

[4] M. Johansson, B. Anderberg, and L.-J. Lindgren, "Magnet design for a low-emittance storage ring", *J. Synchrotron Radiat.*, vol. 21, no. 5, pp. 884–903, Sep. 2014. doi:10.1107/S160057751401666X

[5] A. Wolski, "Maxwell's Equations for Magnets", Jul. 2019. doi:10.48550/arXiv.1103.0713

[6] A. Sharma *et al.*, "Design overview and project status of the PM gradient dipole at MAX IV", Presented at IPAC'26, Deauville, France, May 2026, paper MOP7164, this conference.

[7] Dassault Systèmes, "Opera electromagnetic simulation software". https://www.3ds.com/products/simulia/opera

[8] Dassault Systèmes, "CST Studio Suite". https://www.3ds.com/products/simulia/cst-studio-suite